peer-reviewed version: Russell, R. P., Ocampo, C. A., "Systematic Method for Constructing Earth-Mars Cyclers Using Free-Return Trajectories," Journal of Guidance, Control, and Dynamics, Vol. 27, No. 3, 2004, pp. 321-335.

A SYSTEMATIC METHOD FOR CONSTRUCTING EARTH-MARS CYCLERS USING DIRECT RETURN TRAJECTORIES*

Ryan P. Russell† and Cesar A. Ocampo‡
Department of Aerospace Engineering, The University of Texas at Austin
210 East 24th Street, W. R. Woolrich Laboratories
1 University Station, C0600
Austin, Texas 78712-1085

A procedure for constructing Earth-Mars cycler orbits in a simple solar system is presented. Solutions from the multiple revolution Lambert problem are utilized to find free return Mars trajectories. Multiple combinations of these symmetric return orbits are patched to sequences of full and half-revolution return orbits with Earth-generated gravity-assisted maneuvers. An algorithm is developed to find all useful combinations of direct returns that have a combined period of any integer multiple of the synodic period. Given a sequence of direct returns, a procedure is then developed to minimize the maximum of all the turning angles associated with the flybys necessary to maintain and re-initiate the cycler. The method identifies 24 purely ballistic cyclers with periods of two to four synodic periods, 92 ballistic cyclers with periods of five or six synodic periods, and hundreds of near-ballistic cyclers. These resulting orbits have diverse characteristics that could benefit a variety of potential missions. While the method finds several known cyclers, most of the orbits presented are previously undocumented.

NOMENCLATURE

Symbol	***Description***
a	semi-major axis
AR	Aphelion Ratio
f_j	number of flybys required to re-initiate the j^{th} symmetric return
FR	full-revolution
h	total number of half-years allotted for full or half-revolution direct returns during one cycler period, $h \geq 0$
h_j	total number of half-years allotted for full or half-rev returns associated with the j^{th} symmetric return, $0 \leq h_j \leq h$
i	i^{th} solution, by ascending semi-major axis, from the multiple revolution Lambert problem, $1 \leq i \leq 2N_{MAX}+1$
$INT(\,)$	operator that yields the integer part of its argument
$MOD(\,,\,)$	operator that yields the remainder of the first argument divided by the second argument
N	number of complete revolutions made by a symmetric return, $N \geq 0$
p	The period of the cycler is p synodic periods. $p \geq 1$
r	radius
s	total number of identical symmetric returns during one cycler period, $s \geq 1$
s_j	j^{th} symmetric return
TOF	time of flight for a symmetric return
SR	symmetric return
TR	Turn Ratio
T_{SYN}	synodic period
$\mathbf{v}$	heliocentric spacecraft velocity vector
$\mathbf{v}_\infty$	planet-centered velocity vector before or after flyby
$\mathbf{v}_e$	heliocentric Earth velocity vector
α, β, SP	intermediate variables for Lambert's equation
ϕ, λ	latitude and longitude in reference to the velocity diagrams, see Table 3
γ	heliocentric turning angle
δ	geocentric turning angle
δ_{MAX}	the minimized maximum of $\delta_{MINIMAX\text{-}j}$ for j=1..s
δ_{MIN}	minimum turning angle required to achieve a full-revolution direct return
$\delta_{MINIMAX\text{-}j}$	the minimized maximum turn angle required to re-initiate the j^{th} symmetric return
θ, r_1, r_2, c	input geometry for Lambert's equation, see Figure 1
μ	gravitational parameter

* Presented as Paper AAS 03-145 at the AAS/AIAA Spaceflight Mechanics Meeting, Ponce, Puerto Rico, February 2003.

† Ph.D. candidate. ryanrussell@mail.utexas.edu.
‡ Assistant Professor.

INTORDUCTION

As space exploration advances into the twenty-first century, the development of a sustained human presence on Mars is a reasonable goal in the foreseeable future. Recent[1] interest in cycler orbits as a feasible alternative to the traditional human crewed Mars missions have given researchers new incentive to identify and classify these trajectories. The concept of a cycler trajectory, one that shuttles between two or more celestial bodies, is not new. Several previous studies with favorable results have shown that many such trajectories exist, both ballistic and powered. The purpose of this paper is to combine previous strategies of finding potential cycler orbits into a generalized systematic search. The goal is to use Earth powered gravity-assisted flybys to connect symmetric, half-rev, and full-rev direct return orbits in a logical manner such that the patched trajectory is periodic, requires realistic flybys, and encounters Mars in a simplified solar system.

Recent work by McConaghy[2] et al. found several cycler trajectories using single symmetric return orbits and one cycler using two different symmetric returns. Byrnes[3] showed that energy characteristics of a particular two-synodic period cycler could be considerably improved by including half and full-rev returns. Hollister[4], Rall[5] and Menning[6] used non-linear search methods to find feasible combinations of the full and half-rev direct returns and symmetric returns limited to one revolution. The work presented here combines these approaches into one non-iterative method that scans the defined solution space to identify and classify cycler orbits.

The definition of a cycler and the solar system model is discussed first, followed by a detailed description of the three types of direct returns: full-rev, half-rev, and symmetric. The following two sections discuss the procedure used to re-initiate an identical symmetric return directly or by using intermediate half or full-rev returns. The free parameters associated with each intermediate flyby are then discussed, and a method is outlined to minimize the maximum required turning angle. The next section presents the logic associated with including multiple symmetric returns, followed by a summary of the algorithm, and finally, the results and conclusions. The method reveals many ballistic and near-ballistic cyclers with a variety of time and energy characteristics. Included in the results are the Aldrin cycler[7], the single symmetric return cyclers presented by McConaghy[2] et al, and the two-synodic period cyclers presented by Byrnes[3].

In the context of this paper, the naming convention for the cycler orbits are of the form *p*-*h*-*s*-*i*, where the letters represent four numbers that uniquely identify a class of cyclers. For example, a cycler of the class 4-3-2-12 has a period of 4 synodic periods, includes 3 half-years allotted for full or half-rev returns, and includes 2 symmetric returns using the 12th solution, by ascending semi-major axis, from the multiple revolution Lambert problem. This is a class of cyclers because there are an infinite number of patched trajectories that share these qualities. The order of direct returns and the distinction between full and half-rev is not specified in the naming convention. Table 1 shows the seven different combinations possible for the order of the direct returns for the example given.

Table 1: Possible combinations for direct returns for a cycler with *h*=3 and *s*=2

Number	Sequential Combinations
1	symmetric → symmetric → full-rev → half-rev
2	symmetric → symmetric → half-rev → full-rev
3	symmetric → symmetric → half-rev → half-rev → half-rev
4	symmetric → full-rev → symmetric → half-rev
5	symmetric → half-rev → symmetric → full-rev
6	symmetric → half-rev → symmetric → half-rev → half-rev
7	symmetric → half-rev → half-rev → symmetric → half-rev

Additionally, there are free parameters, described in later sections, associated with each gravity-assisted flyby that patches the direct returns. Therefore, a cycler of the class 4-3-2-12 is uniquely described if the order of the direct returns and all associated free parameters are specified. An algorithm is developed to choose this order and these free parameters such that the required maximum turning angle of all the flybys is minimized given any feasible *p-h-s-i* class of cyclers. The resulting optimized patched trajectory is referenced as *Cycler-p-h-s-i*. The goal then, is to apply the algorithm to the entire solution space of feasible ranges for the variables *p*, *h*, *s*, and *i*. The fixed characteristics of the optimized *Cyclers* are then analyzed and compared. Of particular interest are the resulting cyclers that are entirely ballistic. Once set in orbit, ballistic cyclers require no powered maneuvers to maintain.

CYCLER DEFINITION

A cycler orbit can be generally defined as a perfectly repeatable round-trip trajectory that shuttles between any two or more planets. By definition this is a periodic orbit expressed in any frame that rotates with a period equal to the synodic period. An orbit is periodic in such a reference frame if the initial and final positions and velocities are equal. Additionally, the initial and final relative geometry between all associated bodies must be the same. The later condition is met if the period of the orbit is an integer multiple of the synodic period of the associated planets. Above is the definition of a perpetual cycler and is only a subset of all cycler trajectories. Other non-repeating cyclers may be defined to exist for any sequence of planet encounters, although this paper is restricted only to perpetual cyclers. It is typically desirable to minimize the powered maneuvers required to maintain a given cycler. Depending on the complexity of the solar system model in question, it may be possible to find a completely ballistic cycler. This is defined in this paper to be a repeatable orbit that, once set in motion, encounters two or more planets using only physically allowable gravity-assisted flybys.

SOLAR SYSTEM MODEL

A perpetual cycler with exact repeatability only exists in a very simple solar system model. In the case of the true solar system, it is not feasible to exactly match initial and final conditions and geometries. As a result, solutions must be generated for several decades while simply ignoring the matching end conditions. The obvious extension is to use a true cycler solution from the simple case as an initial estimate for the more complicated model. The current study only addresses the first half of this process. A follow-up study will expand the results to include true ephemerides. The current model chosen is the simplest possible: the circular, coplanar solar system. Although previous studies[4,5] have shown limited success finding true cyclers in a model that includes eccentricity and inclination, the additional complexity and lack of symmetry compels most researchers to use the circular-coplanar model first.

This simple solar system model is defined as follows:

- The Sun is inertially fixed.
- Earth is in a circular orbit with a period of 1 yr. 1 AU =149597870.691 km
- Mars is in a circular and co-planar orbit with a period of 1.875 yrs.
- A zero point patched conic method is used for orbit propagation.
    - Mars provides no gravity-assisted $\Delta\mathbf{v}$'s.
    - Earth is capable of providing instantaneous gravity-assisted $\Delta\mathbf{v}$'s with a zero-radius sphere of influence. μ_{earth} = 3.003489596325074E-006 AU^3/TU^2

Canonical units are used for calculations and defined such that μ_{sun}=1 AU^3/TU^2. The derived time conversion is 1 TU= 58.1324408670490 days. The astronomical unit definition and Earth's gravitational parameter were taken from JPL's DE405 Ephemerides[8]. The period of Mars is chosen such that the absolute geometry repeats every 15 yrs. This value is used to be consistent with previous studies[2,3] and for verification purposes. This value could be changed to 1.8801 yrs., the true period of Mars, and have little effect on the results of this paper. It is assumed that a very minor correction maneuver can be applied to the spacecraft at a great distance to target any altitude for an Earth flyby.

DIRECT RETURN TRAJECTORIES

Timing is crucial in the construction of a cycler. The total cycler period must be an integer multiple of the synodic period. If a spacecraft encounters the Earth prior to the necessary planetary alignment, a direct return may be used to re-encounter the Earth at a later time when the alignment is correct. If the altitude of the required Earth flyby is physically possible, the maneuver requires no fuel.

A direct return trajectory is defined to be any orbit that leaves a celestial body and returns to the same body directly with no powered or gravity-assisted maneuvers. These can be categorized into three general classes of orbits[4,9]. Figure 1 illustrates the half-rev, full-rev, and symmetric direct returns.

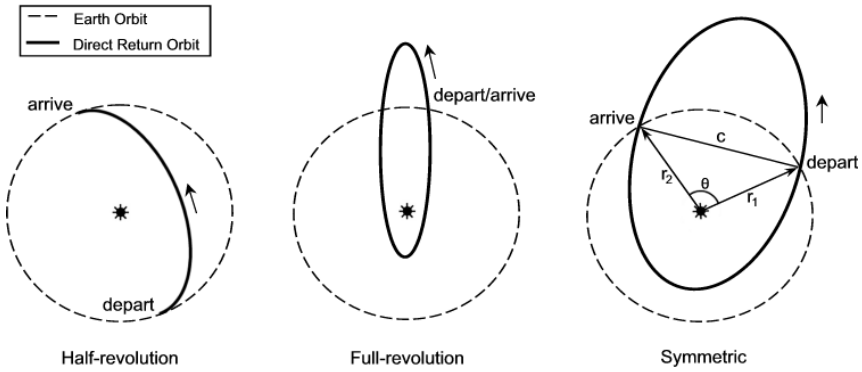

Figure 1: Three types of direct return trajectories

Full-Revolution Direct Returns

For the sake of this paper, the Earth is the planet that generates gravity-assisted maneuvers to patch direct returns orbits, although these principles can be generalized to use any celestial body. The Earth is modeled in this paper as being in a circular orbit; however, the following definitions of direct returns are also valid if eccentricity is included. A full-rev direct return[4] is any orbit that leaves the Earth and returns after the Earth travels exactly one revolution of the Sun. For purposes of this paper, this is the working definition, thus the period of the full-rev direct return is constrained to be the same as that of the Earth. Although technically, the spacecraft will eventually return to the Earth at the same location it departed if the period is any rational multiple of the Earth's period. These unconventional full-rev returns are the subject of further study and will not be investigated here. At departure and arrival, the spacecraft and planet have the same radius from the Sun. If the period of the spacecraft is also the same as that of the Earth, then applying Equation (1), the Energy Equation, it is clear that the velocities must be equal as well. Thus any orbit leaving the Earth with the same heliocentric velocity as the Earth will return after exactly one year.

$$-\frac{\mu}{2a} = \frac{v^2}{2} - \frac{\mu}{r} \tag{1}$$

If a spacecraft approaches the Earth with an arbitrary speed and direction, the geocentric speeds before and after an un-powered flyby are constrained to be equal. The locus of all feasible points for the velocity after a gravity-assisted flyby is the surface of a sphere with radius v_∞ centered at the tip of $\mathbf{v}_e$. The locus of all feasible points where the heliocentric velocity of the spacecraft is the same as that of the Earth is simply a sphere of radius v_e centered at the base of $\mathbf{v}_e$. The intersection of these two spheres, called the full-rev circle, is the locus of all points after a gravity-assisted flyby such that both conditions are met and the spacecraft will return to the Earth after one year. The geometry is illustrated in detail in Figure 2. The profile view is added for clarity. Once a spacecraft is on a full-rev direct return trajectory, it will encounter the Earth each year until a gravity-assisted flyby or any powered maneuver is performed.

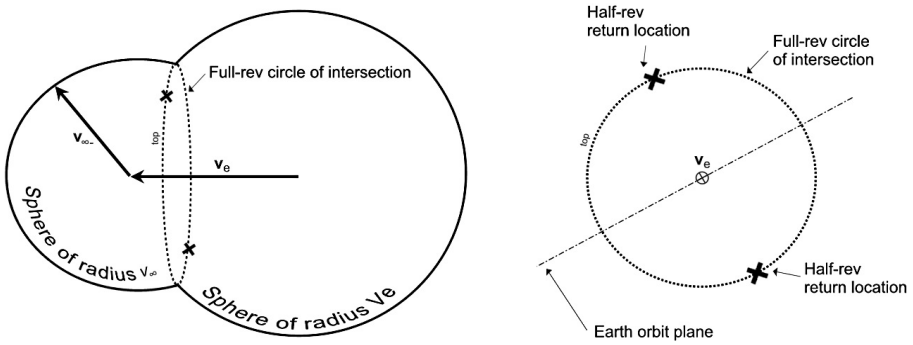

Figure 2: Gravity-assisted flyby velocity diagram

Half-Revolution Direct Returns

A half-rev direct return[4] is any orbit that leaves the Earth and returns after the Earth travels exactly one half-revolution of the Sun. Again, for purposes of this paper, this is the working definition. Technically it is possible to find orbits that will encounter the Earth 180° from its departure after any odd-integer multiple of a half-year. And again, this is the topic of further study. Only times of flight of one half-year will be considered. If a spacecraft leaves the Earth in an orbit with the same semi-major axis and eccentricity as that of the Earth, but with an arbitrary inclination, it will encounter the earth after exactly one half-revolution of the Sun. Figure 1 shows the spacecraft coming out of plane and re-encountering the Earth on the other side. Clearly if no maneuver at Earth is performed, it will re-encounter at the initial departure, making it a full-rev return as well. Therefore, the locus of points creating a half-rev return after an Earth encounter must lie on the full-rev circle of intersection shown in Figure 2. It is known from Gauss' version of the Lagrange planetary equations that a perturbing force perpendicular to the plane of the orbit will not change the orbit's semi-major axis or eccentricity. Therefore, the perturbing force of gravity during a flyby must be perpendicular to the plane of the Earth's orbit in order for the resulting orbit to achieve a semi-major axis and eccentricity equal to that of the Earth. There are two locations on the velocity diagram that are perpendicular to the Earth's orbit plane and also on the full-rev circle of intersection. The above-plane and below-plane locations for these points are marked with an 'X.'

Symmetric Direct Returns

A symmetric return[9], as seen in Figure 1, is characterized by an arbitrary time of flight and any angle of separation between departure and arrival that is not an integer multiple of π. The transfer is therefore limited to be co-planar with the Earth. The name is such because the departure and arrival points are symmetric with respect to the line of apses if the Earth is in a circular orbit. The problem of connecting any two positions with a trajectory of any time of flight is known as Lambert's Problem. It is encountered frequently in astrodynamics and is well documented and understood[10]. Traditional applications involve trajectories that make between zero and one revolution of the primary. However, solutions may exist that make one or more revolutions[10,11,12] if the time of flight is sufficiently large. Generalized to include multiple revolutions, the Lagrangian formulation of Lambert's equation[10] is summarized as the following:

$$\sqrt{u}\ TOF = a^{3/2}\left[2N\pi + \alpha_{short,long} - \beta - \sin(\alpha_{short,long}) + \sin(\beta)\right] \tag{2}$$

where,

$$\sin\left(\alpha_0/2\right) = \sqrt{SP/\left(2a\right)}$$

$$\alpha_{short} = \alpha_0$$

$$\alpha_{long} = 2\pi - \alpha_0$$

$$\sin\left(\beta_0/2\right) = \sqrt{\left(SP-c\right)/\left(2a\right)}$$

$$\beta = \beta_0 \quad \text{if } \theta < \pi$$

$$\beta = -\beta_0 \quad \text{if } \theta > \pi$$

$$SP = 1/2\left(r_1 + r_2 + c\right)$$

Using Equation (2), Figure 3 plots the time of flight vs. semi-major axis for $N = 0..9$. The input geometry for this plot is illustrated by the symmetric return in Figure 1. The curves in Figure 3 represent posigrade solutions, or $0<\theta<\pi$ for this example. A similar plot is obtained for the corresponding retrograde solutions using $\pi<\theta<2\pi$. Notice the time of flight is double valued for each N because of the short and long solutions. In a typical application of Lambert's theorem, the time of flight is given and the corresponding values for semi-major axis are solved iteratively. For a given geometry, an arbitrary time of flight has an associated N_{MAX}. For example, from Figure 3, a time of flight of 20 TU's has an N_{MAX} of 3. Given r_1, r_2, θ, and TOF, an algorithm is developed to identify N_{MAX} and systematically solve for each of the $2N_{MAX}+1$ corresponding values of semi-major axis. Because the algorithm is very similar to the procedure described by Prussing[11], it is not explained in detail. It uses standard root-finding methods to bracket solutions and solve the transcendental equation for semi-major axis. When calculating terminal velocity vectors, a singularity exists if θ is any integer multiple of π because the transfer plane is undefined. Half and full-rev returns are subsets of these cases respectively. In the context of cyclers of the form *p-h-s-i*, the time of flight, expressed in years, for a symmetric return orbit is given by Equation (3). This forces the total period of the cycler to be p synodic periods.

$$TOF = \frac{T_{SYN}\,p - h/2}{s} \tag{3}$$

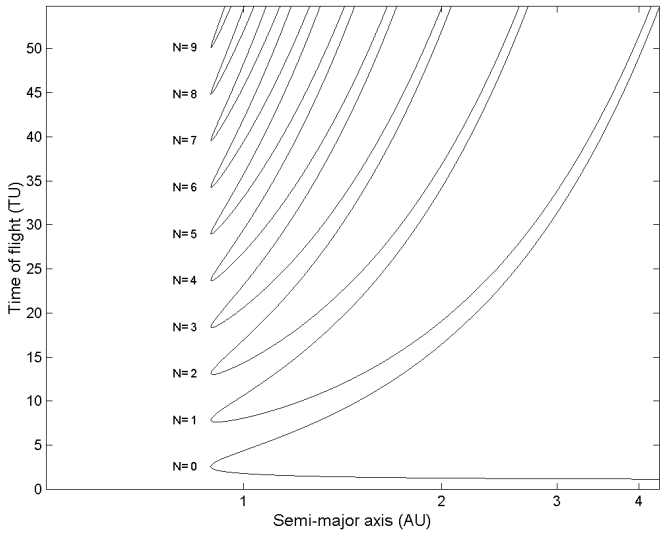

Figure 3: Example multiple revolution Lambert solution (r_1=r_2=1 AU, θ=4π /7)

RE-INITIATION OF AN IDENTICAL SYMMETRIC RETURN

Once a cycler has competed a full cycle, a re-initiation maneuver is necessary to begin the next cycle. This section discusses the conditions required to re-initiate an identical symmetric return using any combination of half or full-rev return trajectories. Figure 4 shows an example of the geometry required to re-initiate a symmetric return trajectory using no intermediate returns.

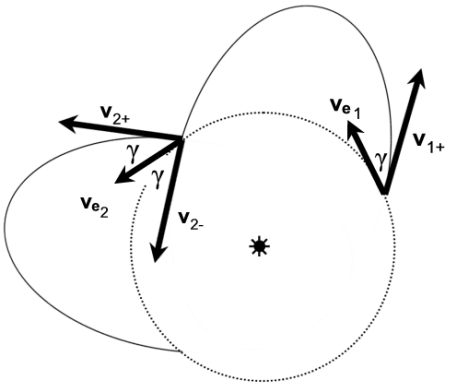

Figure 4: Conditions required to re-initiate symmetric return trajectory

The heliocentric spacecraft velocities at Earth departure and arrival are $\mathbf{v}_{1+}$ and $\mathbf{v}_{2-}$ respectively. Due to symmetry, the magnitudes of these vectors are equal, and the orientation of $\mathbf{v}_{2-}$ with respect to $\mathbf{v}_{e2}$ is a mirror image of $\mathbf{v}_{1+}$ with respect to $\mathbf{v}_{e1}$. The velocity required to re-initiate an identical symmetric return is $\mathbf{v}_{2+}$. Thus, it is clear that the required heliocentric turn angle is 2γ. At t_2 it is also clear that $\mathbf{v}_{\infty-}$ and $\mathbf{v}_{\infty+}$ are coplanar with the Earth's orbit. These conditions apply for the re-initiation of any symmetric return trajectory. The mirror image symmetry can also be seen in Figure 5.

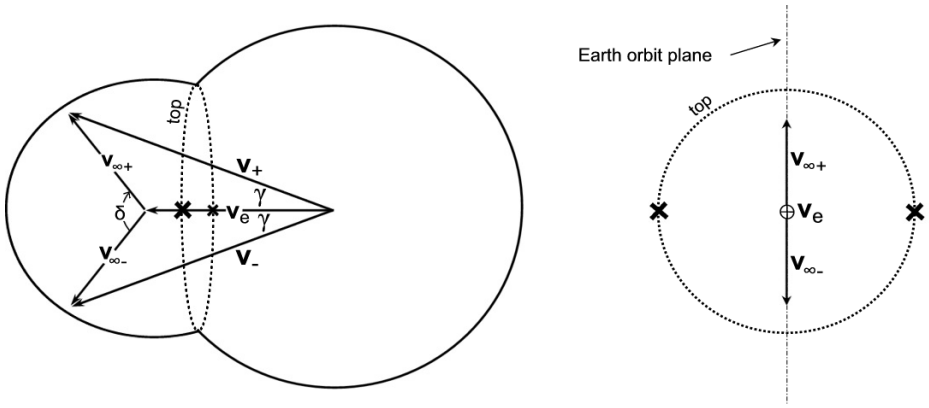

Figure 5: Velocity diagram of a gravity-assisted flyby that re-initiates a symmetric return

If only one flyby is used, Figure 5 indicates that a planar $\Delta\mathbf{v}$ is required to re-initiate the symmetric return. Alternatively, if the timing is not constrained, one or more full-rev direct returns can be performed prior to the re-initiation of the symmetric return. This is possible because the geometry of the velocity diagram remains the same before and after a full-rev return. In order to enter a direct return orbit, the tip of the intermediate $\mathbf{v}_\infty$ must lie somewhere on the intersection of the two spheres on the full-rev circle. Figure 6a shows an example that uses an intermediate full-rev return requiring two flybys to re-initiate the symmetric orbit. The geocentric velocity at the arrival location on a symmetric return is $\mathbf{v}_{\infty 1-}$. The first flyby requires a turn angle of δ_1 in order to place the spacecraft on a full-rev direct return orbit. If no powered or gravity-assisted maneuvers occur, after any integer multiple of years, the Earth and spacecraft return to the same location with the same heliocentric velocities. As a consequence, the velocity

diagram remains unchanged at the time of the second flyby, thus $\mathbf{v}_{\infty 1+} = \mathbf{v}_{\infty 2-}$, and a turn angle of δ_2 is required to achieve $\mathbf{v}_{\infty 2+}$, thus re-initiating the symmetric return. Figure 6b is a similar example requiring three flybys and two intermediate direct return orbits. In these examples, the exact positions of the intermediate $\mathbf{v}_\infty$'s on the dotted full-rev circle are chosen arbitrarily. A following section will discuss a method to optimize the selection of these locations.

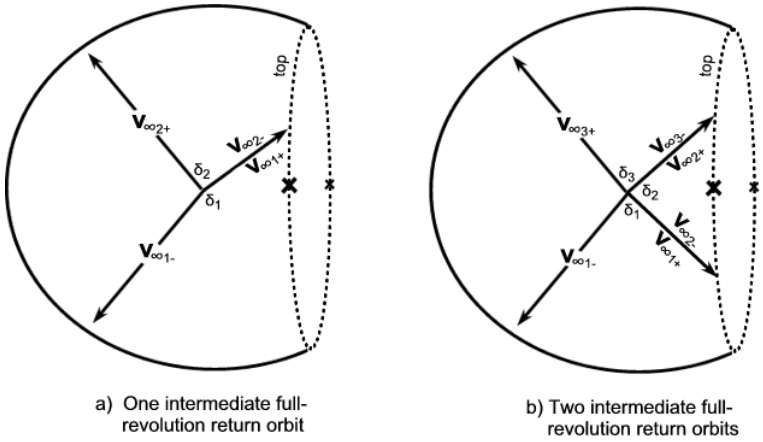

a) One intermediate full-revolution return orbit

b) Two intermediate full-revolution return orbits

Figure 6: Gravity-assisted flyby velocity diagrams with full-rev returns

Consider the example shown in Figure 6a, however choose the location of the intermediate $\mathbf{v}_\infty$ to be the half-rev 'X' above the plane of the paper. This is illustrated in Figure 7a.

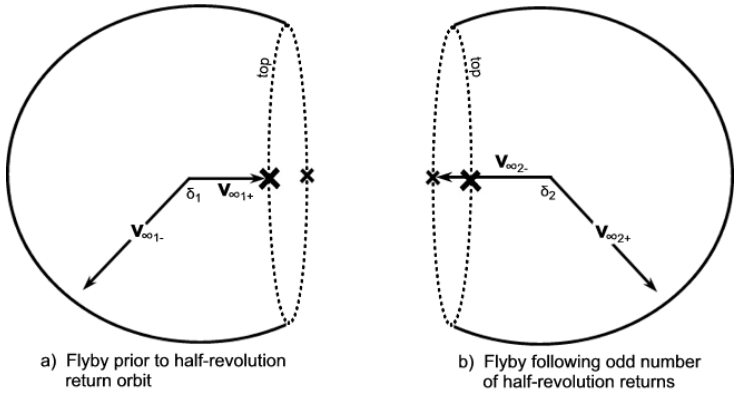

a) Flyby prior to half-revolution return orbit

b) Flyby following odd number of half-revolution returns

Figure 7: Gravity-assisted velocity diagram with half-rev return

Following the first flyby with a turn angle of δ_1 the spacecraft enters a half-rev return trajectory. If no powered or gravity-assisted maneuvers occur, the spacecraft will encounter the Earth after any integer multiple of a half-year. If the next gravity-assisted maneuver occurs after an even number of half-revs, in terms of the velocity diagram, the situation is identical to a full-rev return. However, if it occurs after an odd number of half-revs, then the velocity diagram changes. This is illustrated in Figure 7b. After an odd number of half-revs, $\mathbf{v}_e$, not shown in Figure 6 and Figure 7 but shown in Figure 5, switches directions. Also, the geocentric velocity at the beginning of the half-rev return is opposite of that at the end, or $\mathbf{v}_{\infty 1+} = -\mathbf{v}_{\infty 2-}$. A turn angle of δ_2 is required to achieve $\mathbf{v}_{\infty 2+}$, thus re-initiating the symmetric return. Due to symmetry, it is clear that $\delta_1 = \delta_2$ for this example. Figure 8 combines the two separate diagrams of Figure 7 into one by fixing the direction of $\mathbf{v}_e$ and aligning the respective top and bottom half-rev 'X's. This is equivalent to rotating the diagram in Figure 7b by 180° about an axis perpendicular to the plane of the Earth's orbit, then overlapping the two diagrams. The profile view is included for clarity. Because this view is two-dimensional and easy to illustrate, it will be used frequently for the remainder of this document.

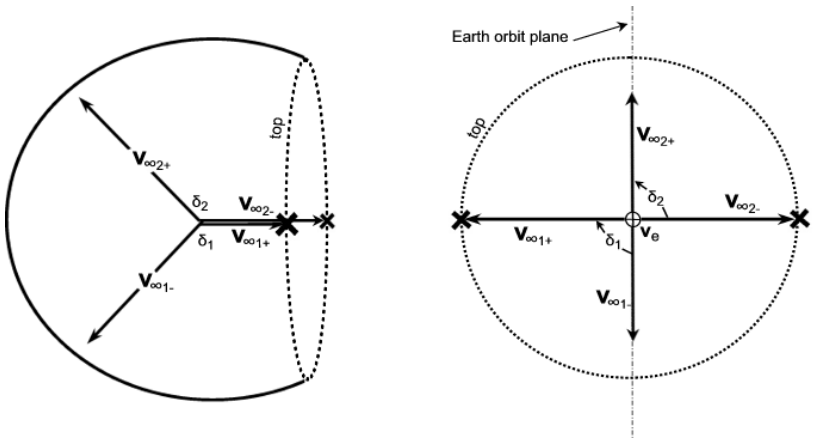

Figure 8: Velocity diagram of a half-rev return with v_e fixed

Turn Angle Optimization for Re-initiation of A Symmetric Return

Thus far, this section has demonstrated how to re-initiate a symmetric return utilizing gravity-assisted Earth flybys that may include full or half-rev return orbits. As mentioned previously, a free parameter is associated with each full-rev return. Additional parameters that are constrained but not fixed are the number of flybys before re-initiation. For example, if a spacecraft is departing Earth on a full-rev return orbit and needs to wait 3 years before re-initiating, should the spacecraft use a gravity-assisted flyby at each of the following Earth encounters, or wait until the third encounter? This is addressed by solving the following optimization problem:

> Minimize the maximum required turning angle necessary to re-initiate an arbitrary symmetric return orbit using any sequence of full or half-rev returns subject to the constraint that exactly h_j half-years elapse before the re-initiation.

Note that the goal is to minimize the maximum required turn angle not the sum of the required turn angles. This is chosen because the primary focus is to find ballistic cyclers. It is acknowledged that a powered cycler[13,14] in the simplified or real model may benefit from minimizing the sum rather than the maximum of the required turning angles. However, in the search for ballistic cyclers in a simple model, the difference is immaterial.

If $h_j=0$, the only option is to immediately re-initiate using one flyby as shown in Figure 5. If $h_j=1$, the only option is to use a half-rev return intermediate flyby before re-initiating as shown in Figure 8. It is arbitrary whether the above or below plane maneuver is used. If $h_j=2$, the options are two half-rev returns or one full-rev return. In the case of using one full-rev return, due to the geometry, the maximum turn angle is minimized if the two turn angles are equal. This serendipitously occurs only if the intermediate $\mathbf{v}_\infty$ terminates at the half-rev 'X.' This is identical to the case of using two half-rev returns. Thus, only two flybys are required when $h_j=2$. If $h_j=3$, the options are to use three half-revs, or one half-rev and one full-rev return. In either case, it is required to have at least one flyby with a turn angle equal to that required when $h_j=1$. It is decided to choose the option that requires fewer flybys in cases when additional flybys do not reduce the maximum required turning angle. Therefore, when h_j=1,2, or 3, two flybys are required (f_j=2), one to navigate $\mathbf{v}_\infty$ from the initial location to the half-rev 'X,' and one to navigate it to the final re-initiation location. Of course the times in between maneuvers are h_j/2 yrs. A similar argument can be made for $h_j \geq 4$. This is summarized in Table 2.

Table 2: Optimal number of flybys necessary to re-initiate a symmetric return

h_j	f_j	Velocity diagram	Time between flybys (yr)
0	1	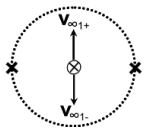	-
1	2	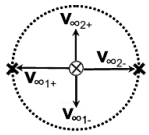	t_2- t_1= ½
2	2	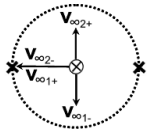	t_2- t_1= 1
3	2	same as h_j =1	t_2- t_1= 3/2
4	3	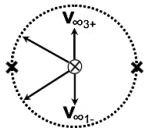	t_2- t_1= 1 t_3- t_2= 1
5	4	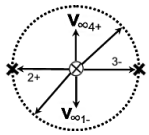	t_2- t_1= 1 t_3- t_2= 1/2 t_4- t_3= 1
6	4	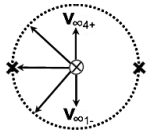	t_2- t_1= 1 t_3- t_2= 1 t_4- t_3= 1
7	4	same as h_j =5	t_2- t_1= 1 t_3- t_2= 3/2 t_4- t_3= 1
8	5	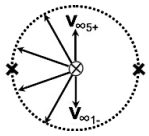	t_2- t_1= 1 t_3- t_2= 1 t_4- t_3= 1 t_5- t_4= 1
⋮	⋮		⋮
h_j even	$h_j/2 + 1$		t_k-t_{k-1} = 1 $\quad k = 2..f$
h_j odd	$2\{\text{INT}(h_j/4 + 1)\}$		t_k-t_{k-1} = 1 $\quad k = 2..(f/2)$ t_k-t_{k-1} = (1/2) MOD(h_j,4) $\quad k = f/2+1$ t_k-t_{k-1} = 1 $\quad k = f/2+2..f$

Once the number of required flybys is known, it is desirable to space them along the full-rev circle in such a manner that the maximum turn angle is minimized. Looking at Figure 5, define a spherical coordinate system using latitude and longitude for the sphere of radius v_∞. The origin of the coordinate system is the center of the sphere. The associated z-axis is aligned with $\mathbf{v_e}$ making the full-rev circle a line of constant latitude. The x-axis is defined such that $\mathbf{v}_{\infty-}$ has only x and z positive components. Figure 9 illustrates this coordinate system with an example that requires five flybys (f_j=5) to re-initiate the symmetric return. The smallest turn angle that ensures a direct return is the flyby that moves $\mathbf{v}_{\infty 1-}$ in the x-z

plane directly along the zero longitude line to the full-rev circle. This angle, δ_{MIN}, is found from Equation (4) and is illustrated in Figure 9a.

$$\delta_{MIN} = \cos^{-1}\left(\cos\phi_{FR}\cos\phi_{SR} + \sin\phi_{FR}\sin\phi_{SR}\right) \tag{4}$$

Depending on the magnitude of this minimum turn angle, there are two cases to consider. If $\mathbf{v}_{\infty 1-}$ is sufficiently far from the full-rev circle, as seen in Figure 9a, then δ_{MIN} is the minimized maximum turn angle. However, if $\mathbf{v}_{\infty 1-}$ is sufficiently close to the full-rev circle, as seen if Figure 9b, then a unique longitude exists, $0 < \lambda < \pi/2$, such that the turning angle, δ_b, is equal for all five flybys. In this case, δ_b is the minimized maximum turn angle.

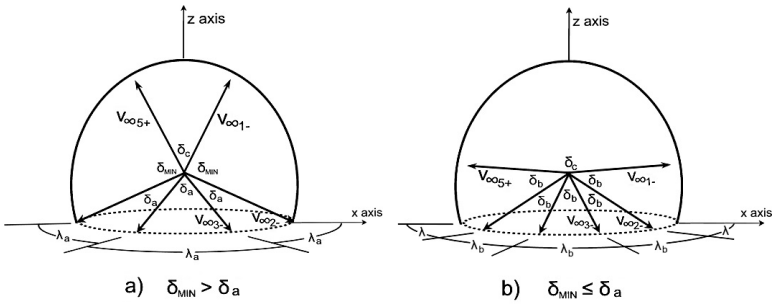

Figure 9: Turn angle optimization for a re-initiation that requires five flybys

The latitudes of the full-rev circle and the symmetric return geocentric velocity vectors are given by Equations (5) and (6).

$$\phi_{FR} = -\sin^{-1}\left[v_\infty / (2v_e)\right] \tag{5}$$

$$\phi_{SR} = \pi/2 - \cos^{-1}\left[\mathbf{v}_{\infty_{1-}}^{\mathrm{T}}\,\mathbf{v}_e / (v_\infty v_e)\right] \tag{6}$$

The turning angles generalized for any $f_j > 2$ are found using Equations (7) – (9).

$$\delta_a = \cos^{-1}\left(\cos^2\phi_{FR}\cos\lambda_a + \sin^2\phi_{FR}\right) \tag{7}$$

$$\text{where} \quad \lambda_a = \pi/(f_j - 2)$$

In order to solve for δ_b, Equation (8) must be solved iteratively for λ. A unique solution exists for $0 < \lambda < \pi/2$ if $\delta_{MIN} < \delta_a$.

$$\cos^2\phi_{FR}\cos\lambda\cos(\lambda_b+\lambda) - \cos\phi_{FR}\cos\lambda\cos\phi_{SR} + \cos^2\phi_{FR}\sin\lambda\sin(\lambda_b+\lambda) + \sin^2\phi_{FR} - \sin\phi_{FR}\sin\phi_{SR} = 0 \tag{8}$$

$$\lambda_b = (\pi - 2\lambda)/(f_j - 2)$$

$$\delta_b = \cos^{-1}\left(\cos\phi_{SR}\cos\phi_{FR}\cos\lambda + \sin\phi_{SR}\sin\phi_{FR}\right) \tag{9}$$

If $f_j = 1$, the turning angle for the only required flyby is δ_c.

$$\delta_c = \pi - 2\phi_{SR} \tag{10}$$

If $f_j = 2$, the turning angle for both required flybys is found by solving Equation (9) with $\lambda = \pi/2$. Equations (4) and (7)-(9) are derived using the known latitudes and longitudes of the vectors that define the turning angles. These coordinates are summarized in Table 3. Equation (8) is derived by setting the angle between $\mathbf{v}_{\infty 1-}$ and $\mathbf{v}_{\infty 2-}$ equal to the angle between $\mathbf{v}_{\infty 2-}$ and $\mathbf{v}_{\infty 3-}$ in Figure 9b. This requires that $\mathbf{v}_{\infty 2-}$ is orthogonal to $\mathbf{v}_{\infty 3-} - \mathbf{v}_{\infty 1-}$.

Table 3: Coordinates for heliocentric flyby velocities

	Figure 9a		Figure 9b	
	latitude	longitude (west)	latitude	longitude (west)
$\mathbf{v}_{\infty 1-}$	ϕ_{SR}	0	ϕ_{SR}	0
$\mathbf{v}_{\infty 2-}$	ϕ_{FR}	0	ϕ_{FR}	λ
$\mathbf{v}_{\infty 3-}$	ϕ_{FR}	λ_a	ϕ_{FR}	$\lambda_b + \lambda$

Due to symmetry, Equations (7) - (10) are still valid if h_j is odd and a half-rev return is required. However, caution is advised when solving for velocities after an odd number of half-rev returns because the velocity diagram switches orientation as indicated in Figure 7.

Given the value of h_j, any arbitrary symmetric return can now be re-initiated using f_j optimized flybys. The calculation of the minimized maximum required turning angle, $\delta_{MINIMAX\text{-}j}$, can be summarized as follows:

1) Calculate δ_c from Equation (10)
2) Get f_j from Table 2
3) IF f_j =1
   $\delta_{MINIMAX\text{-}j} = \delta_c$
   ELSE IF f_j =2
   $\delta_{MINIMAX\text{-}j} = \cos^{-1}(\sin \phi_{SR} \sin \phi_{FR})$
   ELSE IF f_j >2
   Calculate δ_{MIN}, δ_a using Equations (4) and (7)
   IF $\delta_{MIN} \geq \delta_a$
   $\delta_{MINIMAX\text{-}j} = \delta_{MIN}$
   ELSE IF $\delta_{MIN} < \delta_a$
   calculate δ_b using Equations (8) and (9)
   $\delta_{MINIMAX\text{-}j} = \delta_b$

INCLUSION OF MULTIPLE IDENTICAL SYMMETRIC RETURNS

As long as the total period of the cycler is an integer multiple of the synodic period, it is possible for one cycle of a given cycler to consist of multiple symmetric returns. If they are identical, the magnitude of $\mathbf{v}_\infty$ remains unchanged at all of the Earth flybys. As seen in Table 1, the spacing of multiple symmetric returns is a free parameter. This section addresses the logic for choosing this spacing. Given a total number of symmetric returns and half-years allotted for full and half-rev returns, s and h respectively, the purpose of this section is to determine how many half-years, h_j, should be grouped with each symmetric return, s_j. Note that by definition,

$$\sum_{j=1}^{s} h_j = h$$

Once a specific symmetric return is grouped with an optimal number of half-years, the procedure described in the previous section can be applied independently to solve for the best flyby configuration and associated $\delta_{MINIMAX\text{-}j}$ for that grouping. The goal is to minimize the maximum of $\delta_{MINIMAX\text{-}j}$ for j=1..s. The resulting angle is δ_{MAX}. The logic is briefly outlined below:

1) Calculate δ_c, $\delta_{MINIMAX\text{-}j}$ using h_j=INT*(h/s)*
2) IF $\delta_c \geq \delta_{MINIMAX\text{-}j}$
   THEN $h_{1..s\text{-}1}$= INT*(h/s)*
   h_s = INT*(h/s)* +MOD*(h/s)*
   ELSE $h_1 = h$
   $h_{2..s} = 0$
3) $\delta_{MAX} = \delta_{MINIMAX\text{-}1}$

This is derived based on the following observation. If $h_j \geq 1$, $\delta_{MINIMAX\text{-}j}$ will stay the same or decrease if the value of h_j is increased. However for h_j=0, $\delta_{MINIMAX\text{-}j}$ may increase or decrease if the value of h_j is increased, depending on the geometry of the symmetric return. Consider the geometry in Figure 9a. Because $\delta_c < \delta_{MIN}$, it is clear that the maximum required turning angle is lowest if no intermediate direct returns are used. In Figure 9b however, it is clear that additional flybys will lower $\delta_{MINIMAX\text{-}j}$.

As an example, if h=10 and s=3, the two possible cases are {h_1=3, h_2=3, h_3=4} or {h_1=10, h_2=0, h_3=0}. The location of 10 and 4 within respective sets is arbitrary. Note that for h ≥ 1, δ_{MIN} is the lower bound for δ_{MAX}.

ALGORITHM OVERVIEW

An overview of the algorithm is shown in Figure 10. It searches for all cycler solutions with periods from 1 to p_{MAX} synodic periods. A feasible cycler of the form *p-h-s-i* is one whose time of flight for the symmetric return is sufficiently large such that N_{MAX} from Lambert's solution is positive. If N_{MAX} =0, the only solution to Lambert's problem is the Earth's orbit. Also, a negative *TOF* is clearly not a feasible candidate. Equation (3) indicates that *TOF* is indirectly related to *h* and *s*. Therefore, in order to analyze the maximum number of feasible cyclers, it is desirable to choose h_{MAX} and s_{MAX} sufficiently large. The algorithm simply ignores infeasible combinations of *p*, *h*, and *s*.

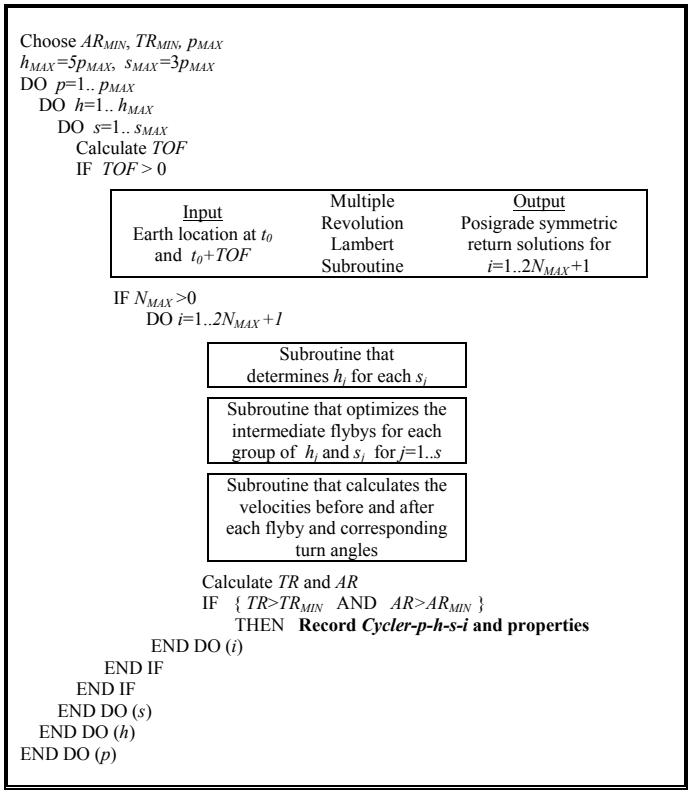

Figure 10: Algorithm Summary

RESULTS

Table 4 lists an example of resulting cyclers using the algorithm described in Figure 10. Each column represents important characteristics to consider when evaluating a particular cycler trajectory. The Aphelion Ratio is the ratio of the maximum ecliptic-plane cycler aphelion radius to 1.52 AU, the radius of Mars. For $AR > 1$, the cycler can intercept Mars without a powered maneuver. The Turn Ratio is the ratio of the maximum physically allowable turning angle to the maximum required turning angle, δ_{MAX}. The maximum allowed turning angle is based on a 200 km altitude Earth flyby. For $TR > 1$, all required flybys are physically attainable without powered maneuvers. Cyclers described in this paper are only guaranteed one Mars encounter each period. Therefore the duration between successive Mars encounters is *p* synodic periods. One approach that increases this frequency is to initiate a new cycler each synodic period. The obvious downside is the cost of each additional cycler vehicle. Thus *p* vehicles are required to ensure a one-synodic period duration between successive Mars encounters. The magnitude of the planet-centered velocities are important primarily because they represent the maneuver requirements to taxi to and from the planets and an existing cycler. The geocentric velocity is also the maneuver requirement to initiate the cycler from Earth. These velocities are inversely related to the duration of the Earth-Mars transit. The

inbound cyclers, although not reported here, have a short Mars-Earth transit instead of Earth-Mars. These are easily found by adjusting the initiating time of the cycler. An additional p vehicles are required to ensure a one-synodic period duration between successive Mars-Earth inbound trips. Due to symmetry, the energy properties for inbound and outbound cyclers are identical[9]. The last column shows the number of gravity-assisted Earth flybys and the geocentric turning angle associated with each one. Depending on the specific needs of a mission, it may be desirable to have a large or small number of flybys.

The AR_{MIN} and TR_{MIN} values used to generate Table 4 are somewhat arbitrary. However, they were selected such that the resulting cyclers would be good candidates for optimization using a more realistic solar system, noting that the true radius of Mars varies from 1.38-1.67 AU. A total of 39 cyclers are shown in Table 4, of which 24 are entirely ballistic. The turn angle optimization described in previous sections is evidenced by the number, order, and values of the turn angles shown in the last column. For example, the two symmetric returns for *Cycler-4-9-2-8* have corresponding h_j's of nine and zero respectively. The first symmetric return is re-initiated using all of the available half-years because the second can be re-initiated using no intermediate returns with only a 24° turn angle. The best configuration for the first re-initiation is to use the δ_{MIN} turning angle of 83° to traverse down to the full-rev circle, followed by four equally spaced maneuvers with turning angles of 44.8°, and finally an 83° maneuver back to the re-initiation location. The velocity diagram for *Cycler-4-9-2-8* is similar to that shown in Figure 9a.

Table 4: Two, three, and four-synodic-period ballistic or near-ballistic cyclers
AR_{MIN}=0.9, and TR_{MIN}=0.9

Cycler-p-h-s-i	*Aphelion Ratio*	*Turn Ratio*	Earth→Mars (or aphelion) Time (days)	Earth v_∞ (km/s)	Mars v_∞ (km/s)	Required Geocentric Turning Angle at each Flyby (deg)							
2- 1- 1- 5[a]	0.95	1.11	207	4.1	2.0	92	92						
2- 3- 1- 5[b]	1.08	0.92	143	5.4	5.3	93	93						
2- 5- 1- 3	1.44	1.12	94	7.8	9.9	54	54	54	54				
3- 1- 1-17	1.07	1.19	174	3.6	4.6	93	93						
3- 1- 2-11	1.07	1.23	181	3.4	4.6	93	93	24					
3- 1- 3- 9	1.43	0.93	123	5.1	9.1	95	95	16	16				
3- 3- 1-15	1.19	1.06	141	4.3	6.8	94	94						
3- 5- 1-11	0.94	1.80	231	2.7	1.5	70	70	70	70				
3- 5- 1-13	1.43	1.15	115	5.4	9.2	73	73	73	73				
3- 5- 2- 9	1.43	1.06	121	5.2	9.2	83	83	83	83	24			
3- 7- 1- 9	1.07	1.56	175	3.6	4.6	71	71	71	71				
3- 9- 1- 7	1.43	1.17	116	5.4	9.2	72	45	45	45	45	72		
4- 0- 3- 7	1.07	1.18	160	4.3	4.9	85	85	85					
4- 1- 1-22	0.94	1.37	256	2.7	1.6	92	92						
4- 1- 1-24	1.15	1.11	173	4.1	6.1	94	94						
4- 1- 2-14	0.94	1.40	250	2.6	1.5	92	92	24					
4- 1- 2-16	1.43	0.93	132	5.2	9.2	95	95	24					
4- 1- 4-10	1.43	0.93	129	5.1	9.2	95	95	12	12	12			
4- 3- 1-20	0.99	1.29	268	3.1	2.5	93	93						
4- 3- 1-22	1.26	1.01	154	4.7	7.6	94	94						
4- 5- 1-18	1.07	1.55	196	3.6	4.7	71	71	71	71				
4- 5- 1-20	1.44	1.15	137	5.5	9.3	73	73	73	73				
4- 5- 2-12	1.07	1.40	191	3.4	4.6	81	81	81	81	24			
4- 5- 3- 8	1.43	1.02	130	5.1	9.2	87	87	87	87	16	16		
4- 6- 1- 3	0.91	1.50	154	6.8	2.1	46	46	46	46				
4- 7- 1-16	1.20	1.38	163	4.3	6.8	72	72	72	72				
4- 7- 1-18	1.77	0.96	120	6.6	11.4	74	74	74	74				
4- 8- 1- 3	0.96	1.64	164	7.7	3.1	37	37	37	37	37			
4- 9- 1-12	0.94	1.83	256	2.7	1.6	69	45	45	45	45	69		
4- 9- 1-14	1.44	1.16	137	5.5	9.3	72	45	45	45	45	72		
4- 9- 2- 8	1.44	1.05	132	5.2	9.2	83	45	45	45	45	83	24	
4-10- 1- 2	0.92	1.46	263	10.2	3.6	30	30	30	30	30	30		
4-10- 1- 3	1.03	1.65	131	8.9	5.0	31	31	31	31	31	31		
4-11- 1-10	1.07	1.58	195	3.6	4.7	70	45	45	45	45	70		
4-12- 1- 2	0.97	1.43	268	11.6	4.8	25	25	25	25	25	25	25	
4-12- 1- 3	1.16	1.48	93	10.8	8.2	27	27	27	27	27	27	27	
4-13- 1- 6	1.44	1.16	137	5.5	9.3	72	30	30	30	30	30	30	72
4-14- 1- 2	1.12	1.13	199	14.7	9.4	22	22	22	22	22	22	22	22
4-14- 1- 3	1.49	1.09	66	14.1	12.7	25	25	25	25	25	25	25	25

[a] "Case 2" cycler described by Byrnes[3]
[b] "Case 3" cycler described by Byrnes[3]

Several of the cyclers presented in Table 4 are worth mentioning. *Cycler-2-5-1-3* is an example of a solution with a relatively short Earth-Mars transit time, perhaps desirable for a human crewed mission. The benefits of the 94-day trip are offset by the relatively high terminal speeds. *Cycler-3-1-1-17*, *Cycler-3-1-2-11,* and *Cycler-3-7-1-9* have low terminal speeds and require 2, 3, and 4 flybys respectively. *Cycler-4-0-3-7* has a transit time of 160 days and relatively good terminal speeds using symmetric returns

only. *Cycler-4-3-1-20* has remarkably low energy requirements at Earth and Mars. The speeds are low because the symmetric return portion of this cycler is very near a Hohman transfer. At Earth, the cycler has a v_∞ of 3.10 km/s compared to the Hohman value of 2.84 km/s, while at Mars the cycler has a v_∞ of 2.53 km/s compared to the Hohman value of 2.57 km/s. The Aphelion Ratio is 0.992, thus the cycler doesn't quite reach Mars in the simplified model. *Cycler-4-5-1-18*, *Cycler-4-5-2-12,* and *Cycler-4-11-1-10* also have promising energy characteristics.

Details about the flyby maneuvers for a few of the discussed solutions are provided in the tables below. They have sufficient data to simulate one complete cycle plus the first leg of the second cycle for each described cycler. The ecliptic is the *x*-*y* axis plane and the initial position of the Earth is always on the *x*-axis.

Table 5: *Cycler-2-5-1-3*

Location	Earth	Mars	Earth	Earth	Earth	Earth	Mars
time (days)	0	94	652	1018	1200	1565	1659
Δv_x (km/s)	6.50[a]	0	-5.19	1.40	-1.40	-5.29	0
Δv_y (km/s)	4.35[a]	0	-1.41	-6.12	6.12	-0.98	0
Δv_z (km/s)	0[a]	0	4.55	3.20	3.20	4.55	0
$\mathbf{r}^T_{mars}$ at $t_0 = [1.41 \quad 0.57 \quad 0]$ AU							

[a]powered Δv required to initiate cycler from Earth

Table 6: *Cycler-3-1-2-11*

Location	Earth	Mars	Earth	Earth	Earth	Mars
time (days)	0	181	1083	1265	2348	2529
Δv_x (km/s)	0.71[a]	0	-0.09	-1.48	-1.28	0
Δv_y (km/s)	3.32[a]	0	-3.59	-3.27	0.62	0
Δv_z (km/s)	0[a]	0	3.39	3.39	0	0
$\mathbf{r}^T_{mars}$ at $t_0 = [1.15 \quad 0.99 \quad 0]$ AU						

[a]powered Δv required to initiate cycler from Earth

Table 7: *Cycler 4-3-1-20*

Location	Earth	Mars[b]	Earth	Earth	Mars[b]
time (days)	0	268	2583	3131	3399
Δv_x (km/s)	-1.24[a]	0	0.18	2.42	0
Δv_y (km/s)	2.84[a]	0	-3.24	-2.16	0
Δv_z (km/s)	0[a]	0	3.09	3.09	0
$\mathbf{r}^T_{mars}$ at $t_0 = [0.93 \quad 1.20 \quad 0]$ AU					

[a]powered Δv required to initiate cycler from Earth
[b]0.008 AU from Mars (cycler aphelion)

Table 8: *Cycler-4-5-2-12*

Location	Earth	Mars	Earth	Earth	Earth	Earth	Earth	Mars
time (days)	0	191	1109	1474	1657	2022	3131	3322
Δv_x (km/s)	-0.71[a]	0	3.38	-3.29	3.29	-1.80	1.29	0
Δv_y (km/s)	3.34[a]	0	-2.86	-0.75	0.75	-4.04	0.62	0
Δv_z (km/s)	0[a]	0	-0.50	-2.91	-2.91	-0.50	0	0
$\mathbf{r}^T_{mars}$ at $t_0 = [1.03 \quad 1.12 \quad 0]$ AU								

[a]powered Δv required to initiate cycler from Earth

Figure 11 shows the top-down view of one cycle of the cyclers presented in Table 7 and Table 5. The dots and numbers sequentially label the planet encounters. A star next to a number indicates a flyby is required. Two stars indicate a flyby that re-initiates the next cycle. Parts c and d illustrate the same trajectories shown in parts a and b, but are plotted in a translating, rotating, and pulsating reference frame[15] that fixes both Earth and Mars for all times. In such a frame, a true cycler orbit is exactly periodic. This frame provides a good measure of periodicity when it is difficult or impossible to find a true cycler, as is the case for the realistic solar system. Parts e and f are zoomed-in on the Earth several orders of magnitude from parts c and d respectively. Note that all half and full-rev returns are out of the ecliptic plane for both cyclers in Figure 11. Additional insight available from the pulsating frame is the visualization of near-encounters with Earth or Mars. As seen in part c, during the symmetric return, the cycler comes very close to a second Mars encounter and moderately close to a third Earth encounter. However, this may be deceiving because the units of distance pulsate by definition in this frame. When expanding the results to include true ephemerides, these additional near-encounters could be constrained to be true-encounters, thus doubling the frequency of successive Earth-Mars transits. The near-Hohman qualities of the Earth- Mars leg are responsible for the near-symmetry seen in part c.

Figure 12 illustrates a 3D view of one cycle of *Cycler-3-1-2-11*. The first leg leaves Earth en-route to Mars via a symmetric return orbit. After 1+ revolutions, an out-of-plane half-rev return connects two Earth flybys, then the second identical symmetric return completes the last leg. The third flyby is required to start the process again. The initial launch $\Delta\mathbf{v}$, the Earth gravity-assisted $\Delta\mathbf{v}$'s, and the times are shown in Table 6.

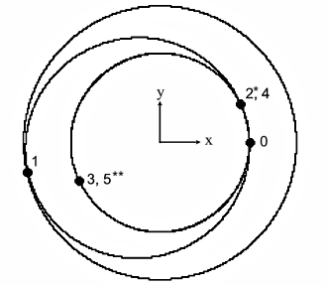

a) *Cycler 4-3-1-20*, Sun-fixed

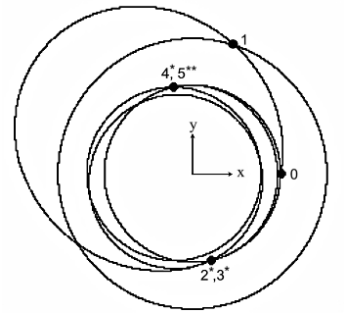

b) *Cycler 2-5-1-3*, Sun-fixed

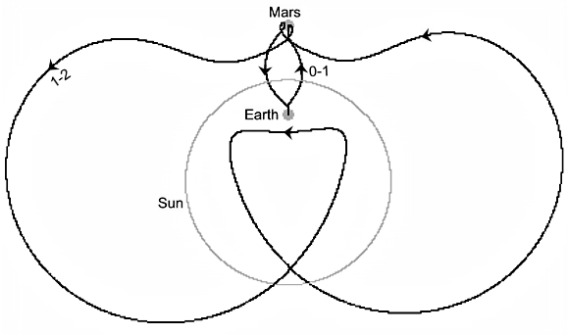

c) *Cycler-4-3-1-20*, Earth/Mars-fixed

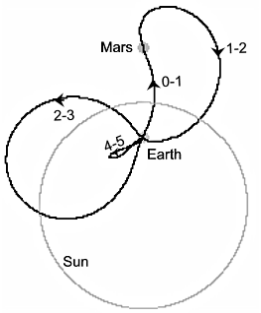

d) *Cycler-2-5-1-3,* Earth/Mars-fixed

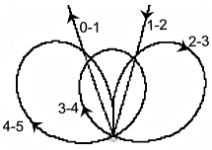

e) *Cycler 4-3-1-20*, near Earth view of c)

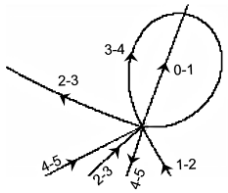

f) *Cycler-2-5-1-3*, near Earth view of d)

Figure 11: Top-down views of *Cycler-4-3-1-20* and *Cycler-2-5-1-3*

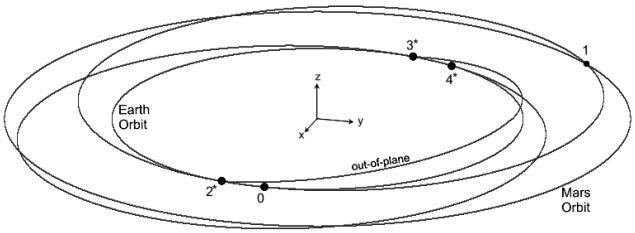

Figure 12: *Cycler-3-1-2-11*

Figure 13 summarizes the number of cyclers found for values of p from 1 to 6. If Table 4 were expanded to include 5 and 6 synodic period cyclers, an additional 149 entries would be added. These are documented in the Appendix. In total, 2502 cyclers are found, 116 of which are totally ballistic and an additional 62 that are close. Cyclers that are integer multiples of previously recorded cyclers are not included in these numbers. For example, *Cycler 4-6-2-5* is not included in Table 4 or Figure 13 because it is simply 2 cycles of *Cycler-2-3-1-5*.

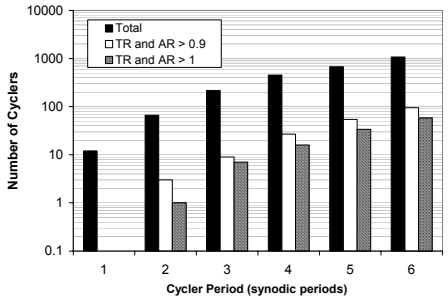

Figure 13: Number of Cyclers Found vs. Period

Some of the cyclers found with this method have been previously documented. *Cycler-2-1-1-5* and *Cycler-2-3-1-5* are identical to the "Case 2" and "Case 3" cyclers described by Byrnes[3]. Although none appear in Table 4, the cyclers found by McConaghy et al[2] are confirmed to be a subset of cyclers presented in this paper with h=0 and s=1. Four of the six-synodic period cyclers are listed in Table A2 in the appendix. *Cycler-1-0-1-6*, with a Turn Ratio of 0.86, is the Aldrin cycler[7].

CONCLUSIONS

A systematic method for constructing ballistic and near-ballistic cyclers between Earth and Mars is presented. The method combines the advantages of previous works into one more generalized approach, utilizing both the geometry associated with direct return velocity diagrams and the many solutions that arise from the multiple revolution Lambert's problem. The method only requires iterations on sub-problems and does not require an initial trajectory estimate. It marches through the entire defined solution space of all feasible combinations of full, half, and symmetric return orbits that combine to form a cycler. Free parameters associated with each unique combination of direct returns are then chosen to minimize the maximum required turning angle, thus maximizing the probability that the cycler is ballistic. Of course, the resulting method is limited by imposed constraints in the problem formulation, thus several extensions are mentioned. The main limitations of the method are that Mars encounters are guaranteed only once during each cycler period, gravity-assist maneuvers are not utilized at Mars or Venus, and the solutions are found using the simplest of solar system models. The method is general in the sense that it encompasses many previously known Earth-Mars cyclers. Additionally, including cyclers with periods of four synodic periods or less, 24 new ballistic cyclers are found. These, along with the many near-ballistic cyclers, exhibit a wide range of energy and time characteristics, making them good candidates for a variety of potential applications.

ACKNOWLEDGEMENT

This work was performed at the University of Texas at Austin supported in part by NASA contract NGT5-141. A special thanks is owed to NASA's Goddard Space Flight Center for providing a Graduate Student Researchers Program Fellowship.

APPENDIX

Table A1: Five-synodic-period ballistic or near-ballistic cyclers
AR_{MIN}=0.9, and TR_{MIN}=0.9

Cycler-p-h-s-i	*Aphelion Ratio*	*Turn Ratio*	Earth→Mars (or aphelion) Time (days)	v_∞ at Earth (km/s)	v_∞ at Mars (km/s)	Required Geocentric Turning Angle at each Flyby (deg)									
5- 1- 1-14	1.04	0.97	229	5.0	4.3	93	93								
5- 1- 2-14	1.20	1.00	168	4.7	7.0	94	94	67							
5- 1- 5- 8	1.44	0.92	133	5.2	9.2	95	95	28	28	28	28				
5- 2- 1- 9	0.90	1.07	182	4.5	1.3	92	92								
5- 2- 2-11	1.20	0.94	128	5.2	7.1	94	94	85							
5- 2- 5- 7	1.43	0.91	118	5.3	9.2	95	95	37	37	37	37				
5- 3- 1-12	0.92	1.17	270	3.8	1.4	92	92								
5- 3- 3-10	1.07	1.19	195	3.6	4.7	93	93	47	47						
5- 4- 1- 7	0.94	1.45	189	4.9	1.9	63	63	63							
5- 4- 1- 9	1.12	1.06	122	7.0	6.3	64	64	64							
5- 4- 3- 7	1.07	1.44	170	3.8	4.7	75	75	75	61	61					
5- 5- 1-10	0.96	1.95	279	4.3	2.2	52	52	52	52						
5- 5- 1-12	1.18	1.44	186	6.2	7.0	53	53	53	53						
5- 5- 1-14	1.48	1.08	154	8.0	10.3	54	54	54	54						
5- 5- 2-10	0.94	1.79	262	3.0	1.7	63	63	63	63	68					
5- 5- 2-12	1.45	1.19	142	5.9	9.5	66	66	66	66	66					
5- 5- 4- 8	1.44	1.10	134	5.3	9.3	78	78	78	78	35	35	35			
5- 6- 1- 7	0.98	1.74	198	5.4	2.7	49	49	49	49						
5- 6- 1- 9	1.20	1.23	107	7.7	7.6	49	49	49	49						
5- 6- 1-11	1.49	0.90	82	9.8	11.0	50	50	50	50						
5- 6- 2- 7	0.94	1.36	219	3.3	1.7	58	58	58	58	86					
5- 6- 4- 7	1.43	1.16	116	5.4	9.2	73	73	73	73	46	46	46			
5- 7- 1-10	1.02	1.78	245	4.8	3.6	52	52	52	52						
5- 7- 1-12	1.30	1.27	169	7.0	8.5	53	53	53	53						
5- 7- 1-14	1.71	0.93	142	9.1	11.9	54	54	54	54						
5- 8- 1- 7	1.03	1.91	154	6.1	4.3	40	40	40	40	40					
5- 8- 1- 9	1.31	1.30	94	8.6	9.1	41	41	41	41	41					
5- 8- 1-11	1.72	0.92	73	11.0	12.6	42	42	42	42	42					
5- 9- 1-10	1.10	2.09	204	5.6	5.7	40	40	40	40	40	40				
5- 9- 1-12	1.48	1.38	154	8.0	10.3	42	42	42	42	42	42				
5- 9- 1-14	2.15	0.93	130	10.5	13.8	45	44	44	44	44	45				
5- 9- 2- 8	1.08	1.57	198	4.0	4.9	60	45	45	45	45	60	67			
5- 9- 3- 6	1.44	1.16	137	5.5	9.3	72	45	45	45	45	72	46	46		
5-10- 1- 7	1.11	1.94	123	6.9	6.2	35	35	35	35	35	35				
5-10- 1- 9	1.49	1.25	82	9.8	10.9	36	36	36	36	36	36				
5-10- 2- 7	1.07	1.71	160	4.3	4.9	59	59	59	59	59	59	59	59		
5-10- 3- 7	1.43	1.24	112	5.7	9.3	66	45	45	45	45	66	60	60		
5-11- 1- 8	1.24	1.76	177	6.6	7.8	41	41	41	41	41	41				
5-11- 1-10	1.83	1.09	138	9.5	12.5	43	43	43	43	43	43				
5-11- 2- 3	1.14	1.00	101	9.6	7.5	47	47	47	47	47	47	47	47		
5-12- 1- 7	1.24	1.81	101	8.1	8.3	32	32	32	32	32	32	32			
5-12- 1- 9	1.82	1.07	70	11.5	13.2	34	34	34	34	34	34	34			
5-13- 1- 6	0.97	2.69	280	4.3	2.3	37	30	30	30	30	30	30	37		
5-13- 1- 8	1.49	1.39	153	8.1	10.3	42	30	30	30	30	30	30	42		
5-13- 2- 6	1.45	1.20	141	5.9	9.5	66	66	66	66	66	66	66	66		
5-14- 1- 3	0.97	3.06	196	5.3	2.6	28	28	28	28	28	28	28	28		
5-14- 1- 5	1.48	1.41	82	9.8	10.9	32	30	30	30	30	30	30	32		
5-14- 2- 5	1.43	1.22	105	6.4	9.5	60	60	60	60	60	60	60	60		
5-15- 1- 4	1.11	2.13	202	5.6	5.8	39	30	30	30	30	30	30	39		
5-15- 1- 6	2.16	0.93	130	10.5	13.9	45	30	30	30	30	30	30	45		
5-16- 1- 3	1.10	2.37	126	6.8	6.0	29	26	26	26	26	26	26	26	29	
5-16- 1- 5	2.12	0.91	64	12.6	14.6	35	25	25	25	25	25	25	25	35	
5-17- 1- 4	1.50	1.37	152	8.1	10.4	42	22	22	22	22	22	22	22	22	42
5-18- 1- 3	1.46	1.45	84	9.6	10.6	32	22	22	22	22	22	22	22	22	32

Table A2: Six-synodic-period ballistic or near-ballistic cyclers

***AR_{MIN}*=0.9, and *TR_{MIN}*=0.9**

Cycler-p- h-s -i	*Aphelion Ratio*	*Turn Ratio*	Earth→Mars (or aphelion) Time (days)	v_∞ at Earth (km/s)	v_∞ at Mars (km/s)	Required Geocentric Turning Angle at each Flyby (deg)											
6- 0- 1-23[a]	0.92	1.40	213	3.0	1.2	86											
6- 0- 1-25[b]	1.03	1.22	179	4.0	3.9	85											
6- 0- 1-27[c]	1.17	1.07	133	5.0	6.7	85											
6- 0- 1-29[d]	1.34	0.93	111	6.0	8.7	84											
6- 1- 2-10	1.09	0.91	203	4.9	5.4	93	93	100									
6- 1- 3- 8	0.95	1.30	264	3.1	1.7	92	92	74	74								
6- 1- 4- 8	1.07	1.16	197	3.8	4.8	93	93	57	57	57							
6- 1- 6- 8	1.44	0.90	135	5.4	9.3	95	95	39	39	39	39	39					
6- 2- 1-21	0.94	1.26	220	3.3	1.7	92	92										
6- 2- 1-23	1.08	1.07	158	4.3	5.0	93	93										
6- 2- 1-25	1.24	0.91	123	5.4	7.6	94	94										
6- 2- 2-17	1.07	1.19	174	3.6	4.6	93	93	47									
6- 2- 3-13	0.94	1.39	235	2.6	1.5	92	92	32	32								
6- 2- 3-15	1.43	0.92	119	5.2	9.2	95	95	31	31								
6- 2- 4-11	1.07	1.23	181	3.4	4.6	93	93	24	24	24							
6- 2- 6- 9	1.43	0.93	123	5.1	9.1	95	95	16	16	16	16	16					
6- 3- 4- 5	1.07	1.04	156	4.5	5.0	93	93	93	93	93							
6- 4- 1-21	0.98	1.59	227	3.6	2.4	70	70	70									
6- 4- 1-23	1.13	1.33	142	4.7	6.0	71	71	71									
6- 4- 1-25	1.33	1.11	113	5.9	8.5	71	71	71									
6- 4- 1-27	1.58	0.93	96	7.0	10.6	72	72	72									
6- 5- 1- 6	0.95	1.62	283	6.2	2.4	47	47	47	47								
6- 5- 1- 8	1.11	1.16	213	8.4	6.6	47	47	47	47								
6- 5- 5- 6	1.44	1.15	137	5.5	9.3	73	73	73	73	46	46	46	46				
6- 6- 1-19	1.02	1.82	189	3.9	3.5	58	58	58	58								
6- 6- 1-21	1.20	1.48	128	5.2	7.1	59	59	59	59								
6- 6- 1-23	1.45	1.21	104	6.4	9.6	60	60	60	60								
6- 6- 1-25	1.78	0.99	89	7.7	11.7	61	61	61	61								
6- 6- 2-15	1.19	1.38	141	4.3	6.8	72	72	72	72	46							
6- 6- 2-17	1.77	0.96	99	6.6	11.3	74	74	74	74	45							
6- 6- 5- 9	1.43	1.03	122	5.1	9.2	85	85	85	85	19	19	19	19				
6- 7- 1- 6	0.98	1.49	289	6.7	3.1	47	47	47	47								
6- 7- 1- 8	1.17	1.05	199	9.1	7.8	47	47	47	47								
6- 7- 2- 3	0.91	0.98	176	5.1	1.5	62	62	62	91	91							
6- 7- 3- 8	1.08	1.40	199	4.1	5.0	62	62	62	62	73	73						
6- 7- 5- 5	1.43	0.99	107	6.1	9.4	62	62	62	62	77	77	77	77				
6- 8- 1-17	0.91	2.39	211	2.9	1.0	51	51	51	51	51							
6- 8- 1-19	1.08	1.89	158	4.3	5.0	53	53	53	53	53							
6- 8- 1-21	1.30	1.50	116	5.7	8.3	54	54	54	54	54							
6- 8- 1-23	1.62	1.18	95	7.2	10.8	55	55	55	55	55							
6- 8- 1-25	2.09	0.94	81	8.6	13.1	57	57	57	57	57							
6- 8- 3-11	1.07	1.47	179	3.4	4.6	77	60	60	60	77	32	32					
6- 9- 1- 6	1.03	1.97	248	7.3	4.5	32	32	32	32	32	32						
6- 9- 1- 8	1.26	1.35	186	10.0	9.1	33	33	33	33	33	33						
6- 9- 1-10	1.57	0.98	161	12.4	12.4	34	34	34	34	34	34						
6- 9- 2- 6	0.96	1.61	274	3.8	2.0	54	54	54	54	67	67	67					
6- 9- 2- 8	1.47	0.94	150	7.2	10.0	56	56	56	56	69	69	69					
6- 9- 4- 6	1.45	1.21	139	5.7	9.4	67	45	45	45	45	67	56	56	56			
6-10- 1-15	0.94	2.31	219	3.3	1.7	50	45	45	45	45	50						
6-10- 1-17	1.15	1.76	137	4.9	6.4	52	45	45	45	45	52						
6-10- 1-19	1.44	1.34	104	6.4	9.6	54	45	45	45	45	54						
6-10- 1-21	1.89	1.02	86	8.1	12.2	56	45	45	45	45	56						
6-10- 2-11	0.94	1.84	231	2.7	1.5	69	45	45	45	45	69	47					
6-10- 2-13	1.43	1.17	115	5.4	9.2	72	45	45	45	45	72	46					
6-10- 4- 9	1.43	1.06	121	5.2	9.2	83	45	45	45	45	83	24	24	24			
6-11- 1- 6	1.09	1.75	219	8.2	6.2	33	33	33	33	33	33						
6-11- 1- 8	1.38	1.17	173	11.0	10.7	33	33	33	33	33	33						
6-11- 2- 3	0.98	1.61	191	6.1	2.9	48	48	48	48	48	48	48	48				
6-12- 1-13	1.00	2.14	232	3.7	2.7	51	36	36	36	36	36	51					
6-12- 1-15	1.26	1.57	120	5.5	7.8	53	36	36	36	36	36	53					
6-12- 1-17	1.67	1.15	92	7.4	11.1	55	36	36	36	36	36	55					
6-13- 1- 3	1.08	0.94	79	16.7	9.7	22	22	22	22	22	22	22	22				
6-13- 1- 4	0.90	3.44	276	5.4	1.5	25	25	25	25	25	25	25	25				
6-13- 1- 6	1.18	1.92	198	9.2	7.9	26	26	26	26	26	26	26	26				
6-13- 1- 8	1.58	1.21	160	12.4	12.5	27	27	27	27	27	27	27	27				
6-13- 2- 6	1.10	1.65	202	5.0	5.4	55	55	55	55	55	55	55	55				
6-13- 3- 6	1.46	1.06	143	6.1	9.6	60	30	30	30	30	30	30	60	72	72		
6-14- 1-13	1.08	1.93	158	4.3	4.9	52	30	30	30	30	30	30	52				
6-14- 1-15	1.44	1.34	104	6.4	9.6	54	30	30	30	30	30	30	54				
6-14- 1-17	2.09	0.94	81	8.6	13.1	57	30	30	30	30	30	30	57				
6-14- 2- 9	1.07	1.59	175	3.6	4.6	70	30	30	30	30	30	30	70	47			
6-14- 3- 7	1.43	1.10	119	5.2	9.2	79	30	30	30	30	30	30	79	31	31		
6-15- 1- 3	1.11	0.90	74	17.2	10.4	22	22	22	22	22	22	22	22				
6-15- 1- 4	0.95	3.00	285	6.3	2.6	25	25	25	25	25	25	25	25				
6-15- 1- 6	1.32	1.57	179	10.5	10.0	26	26	26	26	26	26	26	26				
6-15- 1- 8	1.94	0.94	147	14.3	14.8	28	28	28	28	28	28	28	28				
6-15- 2- 3	1.11	1.27	117	7.7	6.4	39	39	39	39	39	48	48	48	48			
6-16- 1-11	1.20	1.67	128	5.2	7.1	53	26	26	26	26	26	26	26	53			
6-16- 1-13	1.78	1.08	89	7.7	11.7	56	25	25	25	25	25	25	25	56			
6-17- 1- 3	1.14	1.06	69	17.9	11.3	17	17	17	17	17	17	17	17	17	17		
6-17- 1- 4	1.04	2.91	241	7.5	4.8	21	21	21	21	21	21	21	21	21	21		
6-17- 1- 6	1.59	1.24	160	12.5	12.6	26	22	22	22	22	22	22	22	22	26		
6-17- 2- 4	1.48	1.30	149	7.3	10.1	48	45	45	45	45	48	50	50	50	50	50	
6-18- 1- 7	0.94	2.32	219	3.3	1.7	50	22	22	22	22	22	22	22	22	50		
6-18- 1- 9	1.44	1.34	104	6.4	9.5	54	22	22	22	22	22	22	22	22	54		
6-18- 2- 7	1.43	1.17	116	5.4	9.2	72	22	22	22	22	22	22	22	22	72	46	
6-19- 1- 3	1.19	0.97	64	18.8	12.5	17	17	17	17	17	17	17	17	17	17		
6-19- 1- 4	1.20	2.09	195	9.4	8.2	23	22	22	22	22	22	22	22	22	23		
6-19- 2- 3	1.47	1.18	79	10.6	11.1	35	35	35	35	35	35	35	35	35	35	35	35
6-20- 1- 1	0.93	1.09	183	12.8	5.0	29	20	20	20	20	20	20	20	20	20	29	
6-20- 1- 7	1.07	1.94	160	4.3	4.9	52	20	20	20	20	20	20	20	20	20	52	
6-20- 1- 9	2.08	0.94	81	8.6	13.0	57	20	20	20	20	20	20	20	20	20	57	
6-21- 1- 3	1.29	1.01	57	20.3	14.4	14	14	14	14	14	14	14	14	14	14	14	14
6-21- 1- 4	1.63	1.19	158	12.7	12.9	27	18	18	18	18	18	18	18	18	18	18	27
6-22- 1- 5	1.43	1.35	105	6.4	9.5	54	18	18	18	18	18	18	18	18	18	18	54

[a] "Cycler 6S9" described by McConaghy[2] et al.

[b] "Cycler 6S8" described by McConaghy[2] et al.

[c] "Cycler 6S7" described by McConaghy[2] et al.

[d] "Cycler 6S6" described by McConaghy[2] et al.

REFERENCES

[1] Aldrin, Buzz, et al, "Evolutionary Space Transportation Plan for Mars Cycling Concepts," NASA/JPL Contract 1230398, December 15, 2001.

[2] McConaghy, Troy T., Longuski, James M., Byrnes, Dennis V., "Analysis of a Broad Class of Earth-Mars Cycler Trajectories," Paper AIAA-2002-4420, AIAA Astrodynamics Specialist Conference and Exhibit, Monterey, CA, August 2002.

[3] Byrnes, Dennis V., "Analysis of Various Two Synodic Period Earth-Mars Cycler Trajectories," Paper AIAA-2002-4423, AIAA Astrodynamics Specialist Conference and Exhibit, Monterey, CA, August 2002.

[4] Hollister, Walter M., "Periodic Orbits for Interplanetary Flight," Journal of Spacecraft and Rockets, Vol. 6, No. 4, April 1969, pp. 366-369.

[5] Rall, Charles S. "Freefall Periodic Orbits Connecting Earth and Mars," Ph.D. Thesis, Massachusetts Institute of Technology, 1969.

[6] Menning, Michael D. "Freefall Periodic Orbits Connecting Earth and Venus," M.S. Thesis, Massachusetts Institute of Technology, 1968.

[7] Byrnes, Dennis V., Longuski, James M. Aldrin, Buzz, "Cycler Orbit Between Earth and Mars," Journal of Spacecraft and Rockets, Vol. 30, No. 3, May-June 1993, pp. 334-336.

[8] Standish, E. M., "JPL Planetary and Lunar Ephemerides," CD-ROM, Willman-Bell Inc., Richmond, VA, 1997.

[9] Ross, Stanley, "A Systematic Approach to the Study of Nonstop Interplanetary Round Trips," Advances in Astronautical Sciences, Vol. 13. Proceedings of the 9th Annual AAS Meeting, Los Angeles, CA, Jan 1963. pp. 104-164.

[10] Prussing, John E., Conway, Bruce A., "Orbital Mechanics," Oxford University Press, New York, 1993. pp.63-80.

[11] Prussing, John E., "A Class of Optimal Two-Impulse Rendezvous Using Multiple-Revolution Lambert Solutions," Paper AAS 00-250, The Richard H. Battin Astrodynamics Conference, College Station, TX, March 20-21, 2000.

[12] Shen, Haijun, Tsiotras, Panagiotis, "Optimal Two-Impulse Rendezvous Using Multiple Revolution Lambert's Solutions," Paper AIAA-2002-4844, AIAA Guidance, Navigation, and Control Conference and Exhibit, Monterey, CA, August 2002.

[13] Bishop, Robert H., Byrnes, Dennis V., et al, "Earth-Mars Transportation Opportunities: Promising Options for Interplanetary Transportation," Paper AAS 00-255, The Richard H. Battin Astrodynamics Conference, College Station, TX, March 20-21, 2000.

[14] Chen, Joseph K., et al, "Preliminary Analysis and Design of Powered Earth-Mars Cycling Trajectories," Paper AIAA-2002-4422, AIAA Astrodynamics Specialist Conference and Exhibit, Monterey, CA, August 2002.

[15] Ocampo, C., Guinn, J., Breeden, J., "Rendezvous Options and Dynamics for Mars Sample Return Missions," Paper AAS 01-415, AAS/AIAA Astrodynamics Specialists Conference, Quebec City, Quebec, Canada, July 30-August 2 2001.